2023 IEEE/ASME International Conference on Advanced Intelligent Mechatronics (AIM)
June 28-30, 2023. Seattle, Washington, USA

Motion decoupling for cable-driven serial robots based on a noncircular pulley

Jinsai Cheng, Tao Shen

Abstract—Cable-driven serial robots have gained significant growth because of their compact size and low inertia characteristics. However, one major problem of cable-driven serial robots is motion coupling issue that one joint motion will cause movement of the other joints, resulting in a complicated control. In this paper, we proposed a novel method to decouple the joint motion by using a noncircular pulley. The length change of driving cables on a joint pulley due to the coupling issue is compensated by the noncircular pulley. The calculation process of the pulley profile, the mechanical design of the decoupling system, and control system of the cable-driven robot prototype are introduced. Experiments have been conducted to evaluate the performance of the motion decoupling method. The results demonstrate that the noncircular pulley can solve the motion coupling issue by keeping the cable length nearly constant with small errors.

***Index Terms*—Cable-driven, serial robot, motion coupling, motion decoupling, noncircular pulley**

I. Introduction

In the architecture of a serial robot, the output link (also known as the last link/end-effector) is connected to the base link by a single open-loop kinematic chain, which consists of a group of links serially interconnected by revolute or prismatic joints [1]. Because of the single chain structure, the size of the serial robot is relatively compact and often provides a larger workspace as compared to a parallel robot that has several kinematic chains under similar conditions [2]. And, as the architecture of a serial robotic arm is very similar to that of a human arm, the operation of a serial robot will provide the user with a high sense of dexterity [3]. With these advantages, the serial robots are widely applied to different areas such as industries, agriculture, aerospace, and operation rooms [4].

In the medical area, with the help of serial robots, surgeons can obtain greater dexterity, higher precision, better visualization as well as better stability. However, the application of serial robots in the surgical area is usually constrained by space limitations and environmental hazards. First, since surgical robots need to have close contact with human skin or internal organs, a sterilization procedure on the end-effector of the medical robot is indispensable. However, this procedure has a high potential to damage the electronic components of the robot if these components are directly attached to robotic joints [5], [6]. Second, the size of surgical robot needs to be even smaller than the incisions or natural orifices to gain access to the human abdominal cavity [7]. However, the method to use directly motor-driven actuation that has electronic components on the joints is difficult to maintain a compact size and sufficient actuation force [8].

The cable-driven actuation method can be used in serial robots to solve these challenges. By using cable-driven actuation, actuators and electrical sensors can be located far away from harsh environments since the motion and force are transmitted by cables[9], [10]. This relocation of the components can also minimize the size of the robot, and it can also maintain sufficient powers for the robot as remote actuators are not constrained by size. Some current cable-driven serial surgical robots have a continuum or snake-like configuration, which instead of driving robotic joints individually, uses wires to drive all the links or the flexible whole robotic body [11]. Although the continuum/snake-like serial robots are compact and highly hazard-resistant, these robots are under-actuated (i.e., they lack actuation to drive all the joints). The desired trajectories of the manipulator can easily be deflected by the load present at the end link or by any external disturbing force on the robotic body. The biggest challenge in creating a fully actuated rigid-link serial robotic manipulator with a cable-driven method is related to the joint coupling issue. The cables driving the upper joints need to pass through the lower joints. In this case, driving the lower joints will not only rotate the lower joints, but will also affect the movement of upper joints. This decreases the controllability of the robot. Therefore, there is a crucial need to decouple the motion coupling in the cable transmission of serial robots.

Efforts to overcome the motion coupling issues have been made among many researchers. The methods explored by these researchers mainly include software compensation and mechanism compensation methods. Software compensation technique is to develop sophisticate algorithms to compensate the length change of upper joint driving cables due to the motion coupling. Quigley et al. [12] applied a feedforward term in the algorithm to decouple the motion joints in a four-joint manipulator. However, the software compensation method requires accurate and sufficient motion information of the rotation joint, which increases the computational burden of the control system [13]. In addition,

Tao Shen is the corresponding author.
Jinsai Cheng and Tao Shen are with the College of Aeronautics and Engineering, Kent State University, Kent, OH, 44242. (e-mail: jcheng9@kent.edu; tshen3@kent.edu).

it is very challenging to compensate all the joints with motion coupling simultaneously. And lacking precise synchronization in real-time of all the joints, the algorithm methods can create slacking or substantial internal force in the cables which could fail the decoupling [14]. Another type of method focuses on developing novel mechanism structure to compensate the cable length change due to motion decoupling. Glachet et al. [15] developed a parallel bar-linked mechanism to decouple the joints. By using the bar-linked joints, the driving motor has an identical movement as the forearm joint. Thus, the cable length change on one pulley can be absorbed by that on another pulley. However, the size and mass are significantly increased due to the bulky bar linkage structure and the moving motors, and the dynamic performance is also degraded due to the increased mass[13]. Lee et al. [16] developed a decoupling mechanism by adding a moving pulley. When the forearm joint rotates, the moving pulley can move linearly by using a decoupling link to compensate for the cable length change. However, this method can increase the complexity of the cable routing significantly and is prone to errors [17].

In this paper, we present a novel mechanism compensate method based on coupling a noncircular pulley to decouple the motion coupling in rigid serial robots. With this circular pulley, the mechanism is largely simplified, and the system can be kept compact. The detailed design of the structure of the mechanism is introduced. The exploration of the design method is also illustrated in the paper. Experiments have been conducted and demonstrated that there is almost no cable length change of the upper joint driving due to the movement of the lower joint, verifying the effectiveness of the motion decoupling method.

The rest of this paper is organized as follows: The mechanical design and the profile calculation process of the noncircular pulley are described in Section II. The control system of the cable-driven robot prototype is described in Section III. In Section IV, the verification of the performance of the noncircular pulley in length compensation is described.

II. MOTION DECOUPLING DESIGN

A. Motion coupling analysis

In cable-driven serial robots, motion coupling issues are usually caused by cable routing that the cables driving the upper joints need to pass the lower joints, thus the motion of lower joints can affect the rotation of upper joints.

As shown in Fig. 1 (a), three robotic links are connected by a lower joint and an upper joint. The green cable drives the lower joint while the red cable passes through the lower joint and drives the upper joint. Four pulleys are used to route the cables. One pulley is fixed on Link 1 and the other three pulleys are fixed on Link 2. Pulley 2 and Pulley 4 are co-axially attached to the lower joint and upper joint, respectively. The $Arc\ KL$ is the passing-by cable wound on Pulley 2. As the lower joint rotates the angle α clockwise in

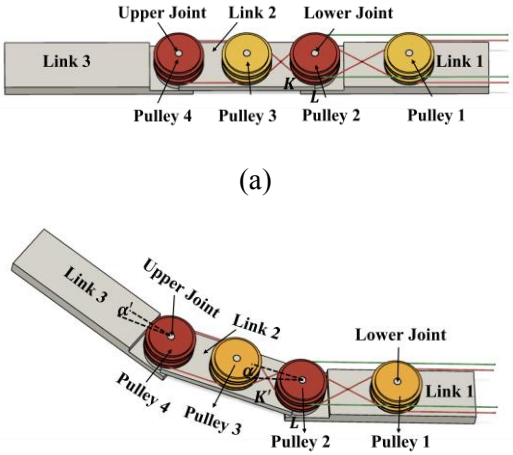

Fig.1. Motion coupling issue (a) Position 1(before rotation) (b) Position 2 (after rotation)

Fig. 1 (b), the $Arc\ KL$ will be changed into $Arc\ K'L$. Thus, the length of the passing-by cable increases and length change can be quantitively denoted as:

$$\Delta l = r\alpha \tag{1}$$

where r is the radius of the joint pulley (Pulley 2), Δl is the length change of the driving cable for the upper joint during the rotation of the lower joint. This length change will cause the upper joint to rotate $\Delta l/r_1$ degree, where r_1 is the radius of the upper joint pulley. From the geometric analysis of the cable, it clearly shows that the lower joint and the upper joint are linearly coupled, which can result in decreased accuracy and reduced performance of the robot.

B. Mechanical design

To solve the motion coupling issue, a rotatable noncircular pulley is proposed to replace Pulley 1 to compensate for the length change. By using this noncircular pulley, the length of the passing-by cable can be kept constant during the movement of the lower joints.

The overview concept of the prototype is shown in Fig. 2 (a). Here we only developed a serial robot with two links and one rotational joint to demonstrate the idea of how the noncircular pulley compensates for the length change. Two fixed guided pulleys are installed on Link 2, and a rotatable noncircular pulley is installed on link 1. Pulley 2 is installed co-axially with the rotational joint. A cable used to drive the upper joint is guided by the three pulleys and passes through the rotational joint. Pin E and Pin F are two guide pins to guide the route of the cable. The cable is fixed on one terminal (left side) on the upper link (Link 2) to simulate driving an upper joint, and another side will be connected to a wire encoder to monitor the change of wire length. As our research is focused on the motion coupling issue, here instead

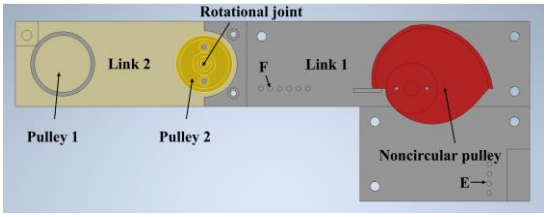

(a)

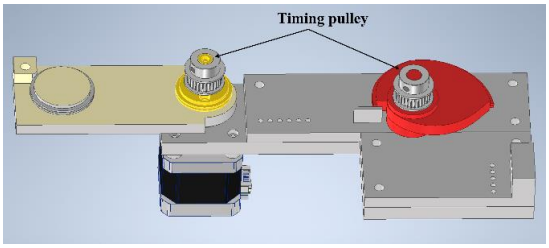

(b)

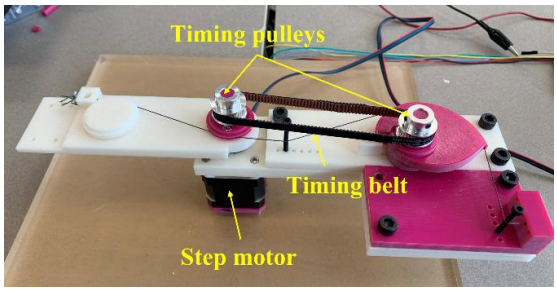

(c)

Fig. 2. (a) Concept design of the cable driving robot (b) Two timing belt used to synchronize the movement (c) The prototype of the cable-driven robot

of using a cable-driven method to drive the rotational joint, we simplify the structure and concentrate on the research problem by using a step motor to directly drive the rotational joint. Therefore, the research problem will be defined as evaluating the length change of the cable while rotating the joint. Once there is no change of cable length during the joint rotation, we can conclude that the proposed method of coupling a noncircular pulley can realize the motion decupling in serial robots. The method we proposed also needs the noncircular pulley to have some movement correlated to the rotational joint. Here we propose the noncircular rotates the same degree as the lower joint synchronously. As shown in Fig. 2 (b), two identical timing pulleys are installed co-axially and fixed on the Pulley 2 and the noncircular pulley, and a timing belt is used to connect the two timing pulleys. Fig. 2 (c) shows the prototype of the cable-driven robot.

C. Noncircular pulley profile calculation

Since the cable length compensation is related to the profile of the noncircular pulley, this section details the calculation process and design of the noncircular pulley profile.

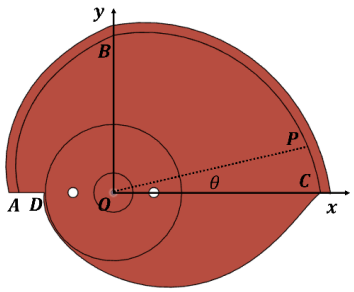

Fig. 3. The profile of the noncircular pulley

Fig. 3 shows the profile of the noncircular pulley, which can be divided into $Arc\ AB$, $Arc\ BC$, Arc CD and line DA. Only $Arc\ AB$ and BC of the noncircular pulley has contact with the cable. Point O is the rotation origin of the noncircular pulley. The $Arc\ BC$ is a predefined shape. The point $P(x_p, y_p)$ on the $Arc\ BC$ can be represented by the following equations:

$$x_p = (l_{OC} - c * \theta) * \cos(\theta) \quad (2)$$

$$y_p = (l_{OC} - c * \theta) * \sin(\theta) \quad (3)$$

where l_{OC} is the length of $Line\ OC$, θ is the angle between

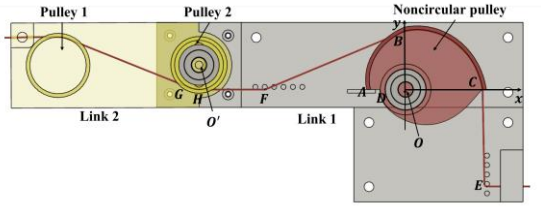

(a)

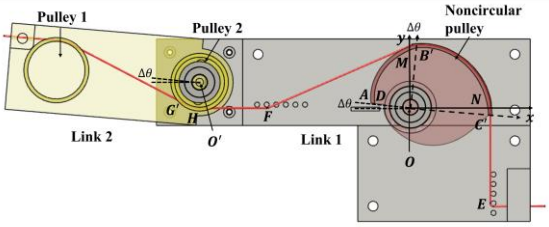

(b)

Fig. 4. Cable routing (a) Cable routing on the robotic links (b) Cable routing after rotation

OP and OC and c is the coefficient to adjust curvature of $Arc\ BC$. When the coefficient is set to 0, then the $Arc\ BC$ is a quarter circle. The $Arc\ AB$ is the noncircular part that needs to be calculated based on the length change during motion.

Fig. 4(a) shows a prototype of a serial robotic link with the installed noncircular pulley and the routing of the cable. The range of motion of the joint is 90 degrees for this prototype.

As the lower joint rotates, the noncircular pulley will rotate by the same degree as the lower joint through the timing belt. After 90 degrees rotation, $Arc\ AB$ will completely replace the original $Arc\ BC$ and become the new contact profile with the cable. So, in this paper, $Arc\ AB$ is the noncircular profile that needs to be calculated. To calculate the profile of the noncircular pulley, the motion is divided into 90 steps. Each step will rotate 1 degree. For each step, the increased length on Pulley 2 will be calculated, and the obtained length change will be used to calculate the noncircular profile of the noncircular pulley on the purpose of countering the length change. The final profile of the noncircular part is obtained by connecting the 90 points.

As shown in Fig. 4 (a), $Arc\ GH$ and $Arc\ BC$ originally are the cables that routed on Pulley 2 and the noncircular pulley, respectively. As the Link 2 rotates around Point O', the cable length increases on Pulley 2. And the length change can be obtained by the following equation:

$$\Delta l_{i1} = r_1 * \Delta\theta \tag{4}$$

where Δl_{i1} is the increased length on Pulley 2, r_1 is the radius of Pulley 2 and $\Delta\theta$ is the rotation angle. The rotation angle for each single step equals to $\frac{\pi}{180}$.

To compensate for the length change, the noncircular pulley will rotate around Point O by the same degree to counter the length increase on $Arc\ GH$. As we can see from Fig. 4 (a), Point B and Point C are the two original endpoints of the driving cable on the noncircular pulley. By setting Point O as the origin point of the coordinate system, Point B and Point C can be described as $(0, l_{\mathrm{OC}})$ and $(l_{\mathrm{OB}}, 0)$, where l_{OC} and l_{OB} is the length of the $Line\ OC$ and OB, respectively. And l_{OB} can be obtained by using (2) and (3). After the noncircular pulley rotates, Point B and Point C will rotate to B', and C', respectively. As shown in Fig. 4(b), two new endpoints M and N of the noncircular pulley that contacted with the cable will replace the original Point B and Point C. And the new Point B' and Point C' can be calculated as follows:

$$B' = \begin{bmatrix} cos\,(\Delta\theta) & sin\,(\Delta\theta) \\ -sin\,(\Delta\theta) & cos\,(\Delta\theta) \end{bmatrix} * [0 \quad l_{\mathrm{OB}}]^T \tag{5}$$

$$C' = \begin{bmatrix} cos\,(\Delta\theta) & sin\,(\Delta\theta) \\ -sin\,(\Delta\theta) & cos\,(\Delta\theta) \end{bmatrix} * [l_{\mathrm{OC}} \quad 0]^T \tag{6}$$

As the noncircular pulley rotates, the cable length of the $Arc\ FB'$ increases compared with the original $Line\ FB$ since the Point B moves away from Point F. The increased length can be described as follows:

$$\Delta l_{i2} = l_{FM} + l_{MB'} - l_{FB} \tag{7}$$

where Δl_{i2} represents the increased length on the noncircular pulley, l_{FM} is the length between Point F and Point M, $l_{MB'}$ is the length of $Arc\ MB'$, and l_{FB} is the length of the original $Line\ FB$.

The cable length of the $Arc\ BC$ becomes the length of $Arc\ B'N$ and the length decreases, which can be obtained by using the following equation:

$$\Delta l_d = l_{OC} * \Delta\theta \tag{8}$$

where Δl_d is the decreased length of $Arc\ BC$, l_{OC} is the length of the $Line\ OC$ as shown in Fig. 4 (a).

The length change of the $Line\ CE$ can be calculated by the following equation:

$$\Delta l_{i3} = l_{NE} - l_{CE} \tag{9}$$

where l_{CE} is the original length of $Line\ CE$, and l_{NE} is the length of the $Line\ NE$. Δl_{i3} depends on the radius of the noncircular pulley in the first quadrant. If the radius is constant, then the cable length of CE is constant. If the radius decreases with a constant coefficient, the length change will increase, and it can be calculated by using (9).

Thus, to make the cable length constant, the increased length and decreased length should be the same, which can be described as follows:

$$\Delta l_{i1} + \Delta l_{i2} + \Delta l_{i3} = \Delta l_d \tag{10}$$

$\Delta l_{i1}, \Delta l_{i3}, \Delta l_d$ can be calculated directly since $r_1, \Delta\theta$, Point N, Point E and Point F have been predefined. Δl_{i2} is related to Point M,which needs to be calculated to form the noncircular profile $Arc\ AB$. Here Point M is constrained on the y axis, and it can be described as:

$$M = (0, y_M) \tag{11}$$

where y_M is the coordinate value of Point M on the axis y.

By using (10), the value of y_M can be calculated. After obtaining the Point M, it will be used as the new Point B for the next iteration.

After calculating Point M, a rotation matrix is applied to transfer Point M to Point M' in the original coordinate:

$$M' = \begin{bmatrix} cos(\Delta\theta) & -sin(\Delta\theta) \\ sin(\Delta\theta) & cos(\Delta\theta) \end{bmatrix} * [0 \quad y_M]^T \tag{12}$$

Since the cable needs to be wrapped on the noncircular pulley, the pulley must be a convex shape with an outwards profile. To ensure that the profile of the pulley is convex, the rate of change of $Arc\ AB$ must monotonically decrease from Point A to Point B.

As shown in Fig. 5, Point M'_{n-1} and Point M'_{n-2} are the calculated points on the $(n-1)$th iteration and $(n-2)$th iteration, respectively. And M_n is the point that needs to be calculated in the current iteration. Since the rate of change of the $Arc\ AB$ needs to monotonically decrease from M'_n to M'_{n-2}, the slope of $M'_nM'_{n-1}$ must be greater than that of $M'_{n-1}M'_{n-2}$. Thus, the point M'_nmust be to the right of the vector $M'_{n-2}M'_{n-1}$. And the following equation can be obtained:

$$y_{m_n} \leq y_{max} \tag{13}$$

where y_{m_n} is the value of Point M_n on the Y axis in the (n)th iteration and y_{max} is the value on the y axis of the

intersection point of the rotated $Line\ M_{n-1}M_{n-2}$ and y axis.

D. Simulation

The radius of the guide Pulley 1 is 13mm. As the joint rotates 90 degrees, the cable length increased on the guide

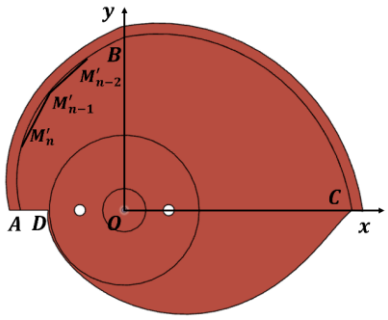

Fig. 5. Discretized points on the profile

pulley is 20.41mm, which can be obtained by using (1). During motion, the noncircular pulley will rotate at the same angle as Pulley 1 to compensate for the length change. To reduce the compensation error, a varying radius of the noncircular pulley in the first quadrant is applied. The l_{OC} is 41mm and the decreasing coefficient is set to 0.11. Thus, the profile of the noncircular pulley in the first quadrant can be obtained using (2) and (3).

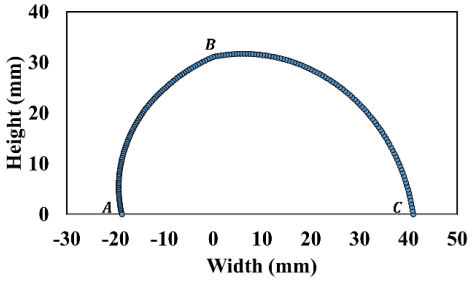

Fig. 6. Profile of the noncircular pulley in the first and second quadrant

By executing the calculation process, the profile of the noncircular pulley in the second quadrant can be obtained. Fig. 6 shows the profile of the noncircular pulley in the first and second quadrant.

E. Error analysis

For each step, the minimal length increase Δl_{i2} is when the Point M is on the line FB'. And the length change can be described as follows:

$$\Delta l_{i2_{min}} = l_{FB'} - l_{FB} \tag{14}$$

If the decreased length Δl_d is smaller than the total minimal increased length, the compensation reaches to the limitation and small error is generated at this iteration, and the intersection of the line FB' and y axis will be directedly used as Point M. The error can be calculated by the following equation:

$$e = \Delta l_{i1} + \Delta l_{i2_{min}} + \Delta l_{i3} - \Delta l_d \tag{15}$$

For each step, the compensation error of the noncircular pulley is shown in Fig. 7. The maximum compensation error is 0.61mm. Compared to the accumulative length increase on Pulley 2 without the noncircular pulley, which is 20.41mm, the length change is within a very small range and has little effect to the upper joint.

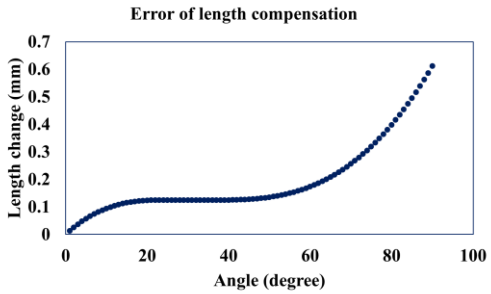

Fig. 7 Errors of length compensation

III. CONTROL SYSTEM

The control system is designed to control the motion of the lower joint and detect the error of the length compensation with the proposed mechanism. The control flow is shown in Fig. 8.

The physical components are shown in Fig. 9. The motion of the lower joint is realized by a step motor, which receives commands from an Arduino Uno and rotates the lower joint to the desired position. The step motor is installed co-axially with a magnet that has 2 poles. A motor driver (A4988, Motor driver, Shenzhen, China) is used to drive the step motor and configured for 800 pulses to make the step motor rotate one revolution. A magnetic encoder is attached to the step motor facing the magnet to detect the actual position with 12-bit high precision. The sensed information by the encoder will be used as feedback for a PID controller, which will compare the desired position with the actual position to achieve accurate motion. To detect the actual length change of the cable-driven system, a wire encoder (CWP-S1000, Wire encoder, Shanghai, China) is used and attached to the one side of the cable. The wire of the encoder can be pull out or retracted automatically. An AD converter (ADS1115, AD converter, Shenzhen, China) with 16-bit resolution is used to capture the voltage change during motion and transfer it to the length change. An Arduino Uno is used and acts as the main controller to control the step motor and capture the data both from the motor encoder and the wire encoder.

The total length of the wire of the wire encoder is 1000

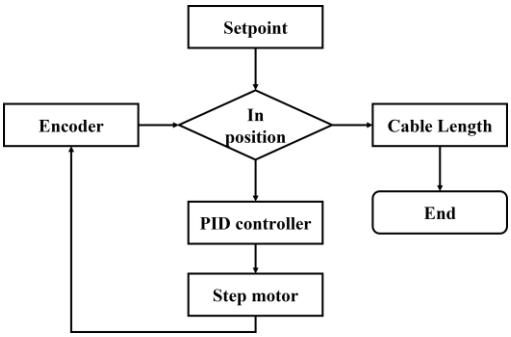

Fig. 8. Diagram of the control flow

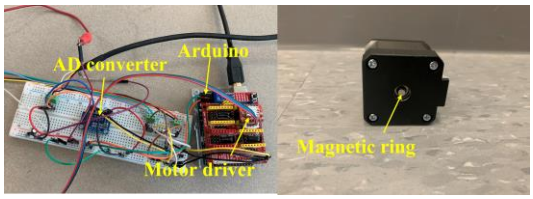

Fig. 9 Control system

mm and the corresponding range of the analog output is from 0 to 5 v. To figure out the relationship between the output voltage and the wire length, a calibration procedure is carried out. The calibration setup is as shown in Fig. 10.

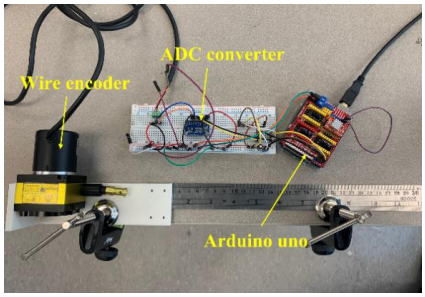

Fig. 10 Calibration of wire encoder

The cable length is measured by a ruler while the output voltage is captured by the AD converter and sent to the Arduino uno. The cable length and the output voltage are recorded during the experiment. Since the length change during motion is small, thus it is unnecessary to figure out the relationship between the full range output and the total cable length. The cable length between 60 mm and 180 mm and the corresponding voltage output are recorded and shown in Fig. 11.

An equation can be obtained by fitting the voltage data and the measured cable length. The following shows the equation of the relationship:

$$l_c = 199.48 * v - 16.98 \qquad (13)$$

where l_c is the cable length and v is the voltage. The length change during motion can be obtained by using the equation.

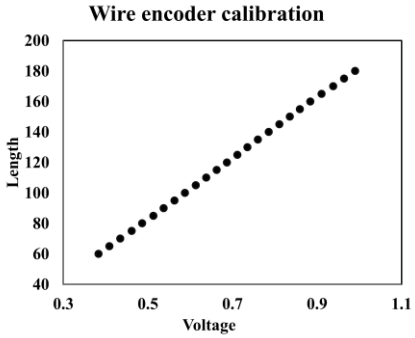

Fig. 11Wire encoder calibration

IV. EXPERIMENT

After assembling the robotic prototype, an experiment was conducted to evaluate the performance of the proposed mechanism. The experiment setup is shown in Fig. 12. The length change of the cable is recorded by the wire encoder.

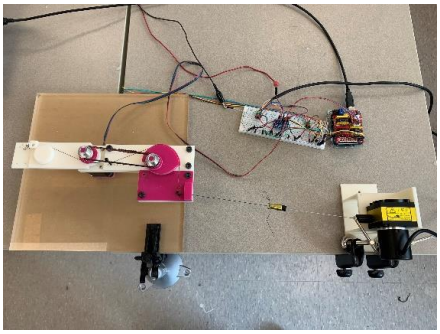
Fig. 12. Length compensation experiment

The lower link starts from the original position and rotates 90 degrees around Point O' to the final position. The motion is divided into 100 steps with 0.9 degree for each step. After each step, the actual position and the cable length change are recorded. Fig. 13 shows the length change during the 90 degrees motion. The orange line shows the length change with a circular pulley, while the blue line shows the length change with the noncircular pulley. As can be shown in Fig.

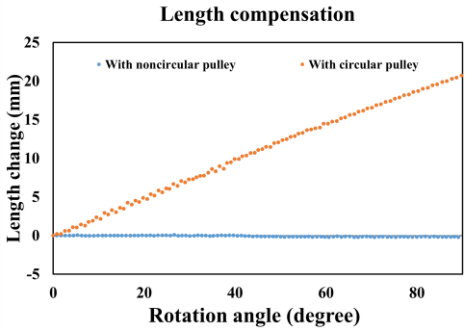

Fig. 13. Length changes during motion

13, the length changes during the entire motion are small with the proposed noncircular pulley. The maximum length change during the motion is 0.22 mm and the average length change is 0.09 mm, respectively. The average and maximum length change are smaller than the simulation results, which may be due to the small variation of component sizes. These results demonstrate that the proposed non-circular pulley can perform good length compensation during motion and can be used to solve the coupling issue of the cable-driven robots.

V. CONCLUSION

In this paper, we proposed a novel method to decouple the joint motion by using a noncircular pulley. The increased length of the cable for driving an upper joint on the lower joint pulley is compensated by decreasing the cable length on the noncircular pulley. The calculation process of the pulley profile is introduced. A mechanism and a control system are developed to demonstrate the effectiveness of the non-circular pully in length compensation. An experiment is conducted, and the results show that the non-circular pulley can compensate for the length change well with a maximum 0.22 mm error and it has a high potential to solve the coupling issue in the cable-driven serial robots.

To improve the performance of the non-circular pulley in length compensation, the future works would continue reducing the length change by applying different parameters.

VI. ACKNOWLEDGEMENT

This material is based upon work supported by the US National Science Foundation under Grant No. 2138903.

VII. REFERENCES AND RESOURCES

[1] L.-W. Tsai, Robot analysis: the mechanics of serial and parallel manipulators. John Wiley & Sons, 1999.

[2] Z. Pandilov and V. Dukovski, "COMPARISON OF THE CHARACTERISTICS BETWEEN SERIAL AND PARALLEL ROBOTS.," Acta Technica Corviniensis-Bulletin of Engineering, vol. 7, no. 1, 2014.

[3] S. K. Mustafa, G. Yang, S. H. Yeo, W. Lin, and I.-M. Chen, "Self-calibration of a biologically inspired 7 DOF cable-driven robotic arm," IEEE/ASME transactions on mechatronics, vol. 13, no. 1, pp. 66–75, 2008.

[4] J. Burgner-Kahrs, D. C. Rucker, and H. Choset, "Continuum Robots for Medical Applications: A Survey," IEEE Transactions on Robotics, vol. 31, no. 6, pp. 1261–1280, Dec. 2015, doi: 10.1109/TRO.2015.2489500.

[5] A. Tzemanaki et al., "Design of a multi-DOF cable-driven mechanism of a miniature serial manipulator for robot-Assisted minimally invasive surgery," Proceedings of the IEEE RAS and EMBS International Conference on Biomedical Robotics and Biomechatronics, vol. 2016-July, pp. 55–60, Jul. 2016, doi: 10.1109/BIOROB.2016.7523598.

[6] Y. Wang, Q. Cao, X. Zhu, and P. Wang, "A cable-driven distal end-effector mechanism for single-port robotic surgery," Int J Comput Assist Radiol Surg, vol. 16, no. 2, pp. 301–309, Feb. 2021, doi: 10.1007/S11548-020-02290-0/FIGURES/13.

[7] A. M. M. Bulbul Chowdhury, J. Cheng, D. Yu, and T. Shen, "Development of a Self-Decoupled Wire-Driven Robotic Universal Joint Toward Medical Application," in Frontiers in Biomedical Devices, American Society of Mechanical Engineers, 2022, p. V001T07A001.

[8] T. Shen, C. A. Nelson, and J. Bradley, "Design of a Model-Free Cross-Coupled Controller with Application to Robotic NOTES," Journal of Intelligent & Robotic Systems 2018 95:2, vol. 95, no. 2, pp. 473–489, Jun. 2018, doi: 10.1007/S10846-018-0836-2.

[9] A. M. Masum Bulbul Chowdhury, M. J. Cullado, and T. Shen, "A Wire-Driven Multifunctional Manipulator for Single Incision Laparoscopic Surgery," Frontiers in Biomedical Devices, BIOMED - 2020 Design of Medical Devices Conference, DMD 2020, Jul. 2020, doi: 10.1115/DMD2020-9015.

[10] A. M. M. Bulbul Chowdhury, J. Cheng, M. J. Cullado, and T. Shen, "Design and Analysis of a Wire-Driven Multifunctional Robot for Single Incision Laparoscopic Surgery," Proceedings of the ASME Design Engineering Technical Conference, vol. 10, Nov. 2020, doi: 10.1115/DETC2020-22471.

[11] T. Shen, C. A. Nelson, K. Warburton, and D. Oleynikov, "Design and Analysis of a Novel Articulated Drive Mechanism for Multifunctional NOTES Robot," J Mech Robot, vol. 7, no. 1, p. 0110041, 2015, doi: 10.1115/1.4029307.

[12] M. Quigley, A. Asbeck, and A. Ng, "A low-cost compliant 7-DOF robotic manipulator," Proc IEEE Int Conf Robot Autom, pp. 6051–6058, 2011, doi: 10.1109/ICRA.2011.5980332.

[13] J. K. Lee, C. H. Choi, H. Yoon, H. J. Lee, S. Park, and J. S. Yoon, "Design and Evaluation of Cable-driven Manipulator with Motion-decoupled Joints."

[14] Y. Liang, Z. Du, W. Wang, Z. Yan, and L. Sun, "An improved scheme for eliminating the coupled motion of surgical instruments used in laparoscopic surgical robots," Rob Auton Syst, vol. 112, pp. 49–59, 2019.

[15] G. J.-P. Glachet C, J. Pontchartrain, and J. Vertut, "Remote manipulator," vol. 817, no. 3, p. 403, Apr. 1973.

[16] J. K. Lee, C. H. Choi, K. H. Yoon, B. S. Park, and J. S. Yoon, "Design of a servomanipulator with tendon transmission," 2008 International Conference on Control, Automation and Systems, ICCAS 2008, pp. 1653–1656, 2008, doi: 10.1109/ICCAS.2008.4694497.

[17] D. Rodriguez-Cianca et al., "The two-degree-of-freedom cable pulley (2DCP) transmission system: An under-actuated and motion decoupled transmission for robotic applications," Mech Mach Theory, vol. 148, p. 103765, Jun. 2020, doi: 10.1016/J.MECHMACHTHEORY.2019.103765.